J Mol Model (2014) 20:2510
DOI 10.1007/s00894-014-2510-3

ORIGINAL PAPER

Physical meaning of the QTAIM topological parameters in hydrogen bonding

Darío J. R. Duarte · Emilio L. Angelina · Nélida M. Peruchena

Received: 21 August 2014 / Accepted: 20 October 2014 / Published online: 5 November 2014

Abstract This work examined the local topological parameters of charge density at the hydrogen bond (H-bond) critical points of a set of substituted formamide cyclic dimers and enolic tautomers. The analysis was performed not only on the total electron density of the hydrogen bonded complexes but also on the intermediate electron density differences derived from the Morokuma energy decomposition scheme. Through the connection between these intermediate electron density differences and the corresponding differences in topological parameters, the meaning of topological parameters variation due to hydrogen bonding (H-bonding) becomes evident. Thus, for example, we show in a plausible way that the potential energy density differences at the H-bond critical point properly describe the electrostatics of H-bonding, and local kinetic energy density differences account for the localization/delocalization degree of the electrons at that point. The results also support the idea that the total electronic energy density differences at the H-bond critical point describe the strength of the interaction rather than its covalent character as is commonly considered.

Keywords Energy decomposition · QTAIM · Morokuma · Hydrogen bonds · Difference density

Electronic supplementary material The online version of this article (doi:10.1007/s00894-014-2510-3) contains supplementary material, which is available to authorized users.

D. J. R. Duarte (✉) · E. L. Angelina · N. M. Peruchena
Laboratorio de Estructura Molecular y Propiedades, Área de Química Física, Departamento de Química, Facultad de Ciencias Exactas y Naturales y Agrimensura, Universidad Nacional del Nordeste, Avda. Libertad 5460, 3400 Corrientes, Argentina
e-mail: djr_duarte@hotmail.com

Introduction

Originally, the hydrogen bond (H-bond) was considered an electrostatic interaction, as evidenced by previous definitions stating that H-bonds could be formed only when the hydrogen atom is placed between the most electronegative atoms [1]. However, it has been recognized gradually that other types of energetic contributions, such as charge transfer and dispersion energies, are also relevant to H-bond formation. Recently, Grabowski [2] stated that many lines of evidence converge on recognition of the unique importance of covalency (charge transfer) in the general H-bonding phenomenon.

The decomposition of interaction energy (or energy decomposition analysis, EDA) is useful when analyzing H-bonding and particularly to answer the question of whether H-bonding is an electrostatic or covalent interaction [2]. Interaction energy decomposition schemes describe H-bonding phenomena in terms of energy contributions, i.e., electrostatic, polarization, exchange-repulsion, charge transfer and dispersion components. In a Morokuma-like decomposition scheme [3, 4], the total interaction energy is decomposed into the following components:

$$E_{ES} + E_{PL} + E_{EX} + E_{CT} + E_{DISP} = E_{TOT} \quad (1)$$

from left to right: electrostatic, polarization, exchange-repulsion, charge transfer and dispersion. These components are obtained by neglecting some elements of the Fock and overlap matrices of the constituent fragments, and then solving the Hartree-Fock equation self-consistently [4].

The major problem with the concept of binding energy decomposition or total interaction energy decomposition is that only the total interaction energy is a physical observable. The various proposed components, while they might seem intuitively reasonable, are not defined uniquely and cannot be determined experimentally [5]. Furthermore, many of the

components are not independent of each other, and any attempt to separate them is artificial. For instance, an electrostatic interaction between two molecules intrinsically involves some degree of mutual polarization. In this sense, polarization (E_{PL}) is part of the electrostatic component (E_{ES}) [6].

In an analogous manner, when the sharing of electrons between monomers is "switched on" within the EDA, two components of the interaction energy come in to play simultaneously: the charge transfer (E_{CT}) and the inter-electronic repulsion (E_{EX}) between the monomers. Keeping in mind the above concepts, in a previous work we decomposed the complex interaction to a minimal degree, giving rise to only two meaningful terms: the ($E_{ES} + E_{PL}$) term that can be related to the "purely electrostatic part" of the interaction energy, and the ($E_{EX} + E_{CT}$) term that accounts for the "sharing of electrons" between the monomers [7].

On the other hand, in the context of quantum theory of atoms in molecules (QTAIM) [8], the topological parameters of the charge density provide the characteristics at the H-bond critical point. Through the local statement of the virial theorem (Eq. 2), a property of the charge density, as its Laplacian ($\nabla^2\rho_b$), can be related to the local kinetic energy density (G_b) and the local potential energy density (V_b).

$$_{1/4}\nabla^2\rho_b = 2G_b + V_b \quad (2)$$

Because $G_b>0$ and $V_b<0$, the modulus of the potential energy ,outweighs two times the kinetic energy, in those space regions with electronic charge concentration, i.e., where $\nabla^2\rho_b<0$.

Moreover, the local electronic energy density at the interaction bond critical point (BCP) is given by

$$H_b = G_b + V_b \quad (3)$$

While these local energy densities have a well defined physical meaning, interpretation of the variation of these quantities in the context of H-bond formation is not as clear as it should be. The previous statement is supported by the current controversy around the meaning of H_b negativity [7, 9]. One can see from Eqs. 2 and 3 that, for regions with electronic charge concentration where $|V_b|>2\ G_b$, the local electronic energy density will be also negative. Therefore, a negative value of H_b is often interpreted as a consequence of the charge density accumulation at the interaction BCP [10–13]. Based on the previous statement, Grabowski et al. [14] established that it is possible to observe three H-bonding regions: (1) covalent [r(H···Y)<1.2 Å], (2) partially covalent [r(H···Y) between 1.2 and 1.8 Å] and (3) noncovalent [r(H···Y)>1.8 Å] wherein the topological parameters characteristic or these three regions are, respectively, $\nabla^2\rho_b$ and $H_b<0$, $\nabla^2\rho_b>0$ but $H_b<0$, and both $\nabla^2\rho_b$ and $H_b>0$. Thus, a negative value of H_b is associated with covalency.

However, we have a different interpretation around the meaning of H_b negativity. In previous works [7, 9], we studied halogen and hydrogen bonding complexes with the aim of understanding the nature of such interactions and asked the following question: is the decrease in the total electron energy density a covalence indicator in hydrogen and halogen bonds? On this issue, the QTAIM theory in conjunction with reduced variational space self-consistent field (RVS) EDA was employed. Through combining both methodologies, it was possible to provide a different interpretation for H_b as a local electronic energy density that can be decomposed in two local energy densities, ($-G_b$) and ($¼\nabla^2\rho_b$), that are connected via the ($E_{ES} + E_{PL}$) and ($E_{EX} + E_{CT}$) terms of the total complex interaction energy, respectively. By applying the proposed decomposition scheme to a set of hydrogen and halogen bonding complexes, it was found that the decrease in H_b toward negative values as the interaction strengthens is due mostly to the increase in the electrostatic contribution to the total interaction energy. In a recently published work on boron-based complexes with carbene as an electron donor [15], the authors found that the SAPT electrostatic energy correlates well with the H_b value, therefore supporting our results.

This kind of study on the interrelationship between QTAIM topological parameters and interaction energy components, pioneered by Grabowski and his collaborators [14, 16, 17], seems to be a good strategy with which to investigate the meaning of the charge density topological parameters. However, one should be aware that such analysis might not be entirely correct since the components of the interaction energy and the local topological parameters are measured on different electron densities (the former were obtained from the various intermediate electron densities derived from the EDA analysis while topological parameters were measured on the total electron density of the complex).

With that in mind, by using a different approach, we present a study of the local topological parameters, focusing not only on the total electron density of the complex but also on the intermediate electron densities differences derived from the Morokuma energy decomposition scheme in order to gain insight into the meaning of the variation of the local topological parameters in the context of H-bond formation. This study was carried out on a set of substituted formamide cyclic dimers $(FD\text{-}X)_2$ and enolic tautomers $(FA\text{-}X)_2$ (see Scheme 2 below).

Computational details

The H-bonded complexes were optimized at the MP2/6-311++G(d, p) level of calculation. The harmonic vibrational frequencies were calculated with analytic second derivatives at the same level, which confirmed that the structures were

minima. All these electronic structure calculations were performed with the Gaussian 03 suite of programs [18].

After the complexes were optimized, the interaction EDA [3, 4], as implemented in the GAMESS quantum chemistry package [19], was carried out at the MP2/6-311G(d,p) level of theory. In addition to the energy components, the corresponding intermediate electron densities were also extracted from the decomposition analysis. Calculation of local topological properties of the electron charge density was performed for each of the intermediate densities employing the AIMAll package [20], and molecular graphs as well as contour maps were displayed.

Scheme 1 shows how the total charge density of the H-bonded complexes $\rho^{MP2}(m_1,m_2)$ can be constructed from the intermediate electron densities derived from the Morokuma analysis.

In the initial step, the charge densities from the isolated monomers were placed together in the complex geometry, $[\rho(m_1) + \rho(m_2)]$. Then, each monomer was allowed to distort internally under the electric field of the other monomer, $\rho(m_1^*, m_2^*)$. The difference between the distorted $\rho(m_1^*, m_2^*)$ and undistorted $[\rho(m_1) + \rho(m_2)]$ charge density accounts for the polarization or internal redistribution of the electronic charge within each monomer. Since the electronic redistribution in this step does not involve sharing of electrons between the monomers, it is named $\Delta\rho_{ncov}$ for non-covalent. In the next step, the sharing of electrons between monomers is allowed (i.e., differential overlap between monomers is permitted). The resulting charge density difference, $\Delta\rho_{cov}$, recovers the interelectronic repulsion (EX) and the charge transfer (CT) between the monomers due to the intermolecular overlap. Finally, the difference between the Hartree-Fock and the MP2 total charge densities, $\Delta\rho_{disp}$, accounts for the effect of the electron correlation in complex formation.

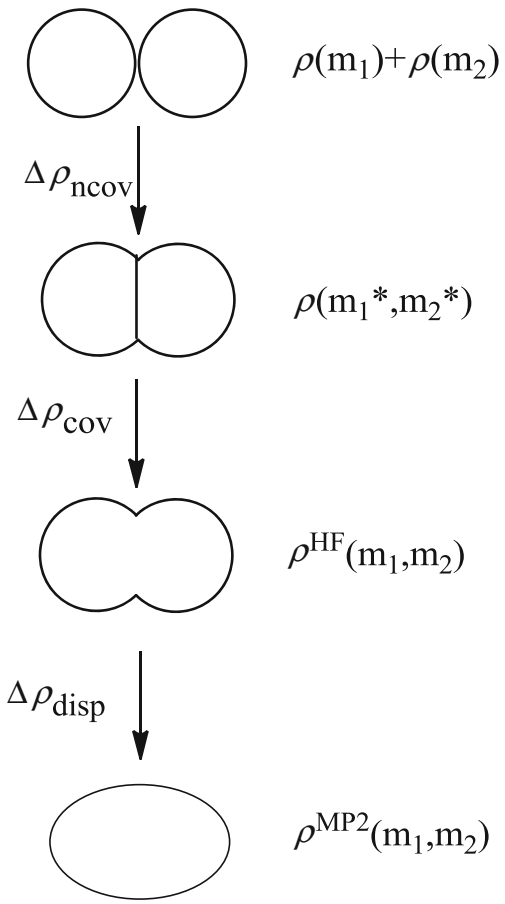

Scheme 1 Construction of total charge density of the H-bonded complexes ρ MP2 (m1 , m2) from intermediate electron densities derived from Morokuma analysis

Results and discussion

Scheme 2 shows the cyclic dimer of formamide $(FD\text{-}X)_2$ and its enolic tautomer $(FA\text{-}X)_2$, i.e., the formamidic acid cyclic dimer, where the non interacting hydrogen atom bonded to the nitrogen has been replaced by various groups of different electron-withdrawing/donating capacity in order to modify the H-bond strength. In this way, we were able to study the variation of the different components of the total interaction energy (E_{TOT}) as a function of H-bond length.

Figure 1 shows the variation in the interaction energy components as a function of the H-bond length in the substituted formamide cyclic dimers and their tautomeric counterparts.

From Fig. 1 it can be seen that the N···H H-bond distance in the $(FA\text{-}X)_2$ dimers is shorter than the O···H H-bond distance in the $(FD\text{-}X)_2$ dimers. Moreover, on going from the $(FD\text{-}X)_2$ to $(FA\text{-}X)_2$ dimers, the components E_{ES}, E_{PL}, E_{CT} and E_{DISP} become more negative and the exchange repulsion (E_{EX}) increases its positive value. As the sum of the negative components grows faster than the E_{EX} component, the total interaction energy (E_{TOT}) increases its negative value

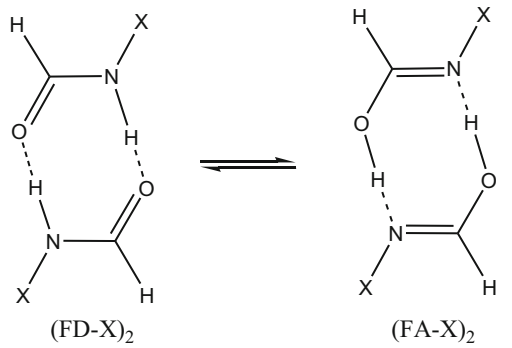

X = H, CN, CHO, NH_2, NO, OH, F, Cl, CH_3

Scheme 2 Cyclic dimer of formamide $(FD\text{–}X)_2$ and its enolic tautomer $(FA\text{–}X)_2$

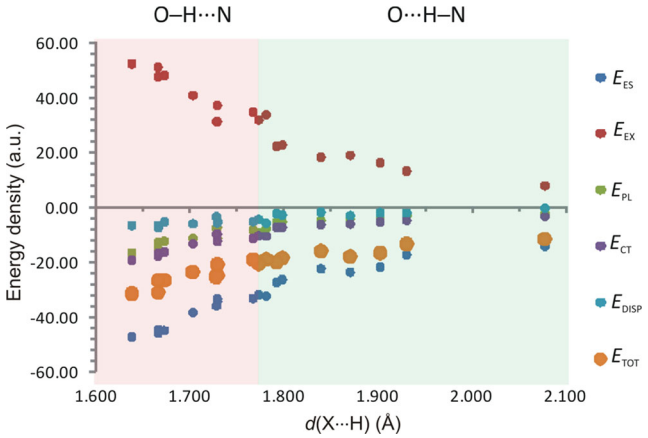

Fig. 1 Variation of interaction energy components as a function of the O···H and N···H H-bond distances in $(FD\text{-}X)_2$ and $(FA\text{-}X)_2$ dimers, respectively

as the H-bond shortens (i.e., complexes become more stable), reaching the most negative values in the $(FA\text{-}X)_2$ complexes.

On the other hand, the local topological parameters of the charge density provide the characteristics of the interaction at the H-bond critical point. Table 1 shows the local topological parameters at one of the two equivalent H-bond critical points of the $(FA\text{-}X)_2$ complexes. From now on, the discussion is focused on $(FA\text{-}X)_2$ complexes, though the results also apply to their tautomeric counterparts, $(FD\text{-}X)_2$.

As is evident from the H-bond distance [d(H···Y)] as well as the charge density value at the H-bond critical point (ρ_b) (Table 1), the fluorine- and amino-substituted dimers present the weakest H-bonds whereas the formyl-substituted complex has the strongest bond, with intermediate ρ_b values for the other substituents. It is also noted from Table 1 that all the complexes share a positive value of the Laplacian of the charge density ($1/4\nabla^2\rho_b$) but a negative value of the total electronic energy density (H_b) at the H-bond critical point. Furthermore, $1/4\ \nabla^2\rho_b$ in general decreases and H_b increases in magnitude on going from the weakest to strongest substituted dimer.

Table 1 Local topological parameters [in atomic units (a.u.)] of the charge density calculated on the total correlated electron charge density of $(FA\text{-}X)_2$ complexes. H-bond distance (in Å) as a function of the substituent X is shown

X	d(H···Y)	$\rho^{MP2}(m_1,m_2)$				
		ρ_b[a]	$1/4\ \nabla^2\rho_b$	G_b	H_b	V_b
F	1.773	0.0431	0.0267	0.0326	−0.0059	−0.0385
NH_2	1.781	0.0435	0.0260	0.0322	−0.0062	−0.0384
OH	1.767	0.0447	0.0264	0.0333	−0.0069	−0.0402
CN	1.729	0.0483	0.0262	0.0354	−0.0092	−0.0445
Cl	1.703	0.0513	0.0277	0.0384	−0.0107	−0.0491
H	1.673	0.0559	0.0267	0.0405	−0.0138	−0.0544
NO	1.666	0.0571	0.0259	0.0407	−0.0148	−0.0554
CH_3	1.666	0.0582	0.0259	0.0414	−0.0155	−0.0569
CHO	1.638	0.0614	0.0254	0.0431	−0.0178	−0.0609

[a] The b subscript indicates that the topological properties have been measured at one of the two equivalents H-bond critical points from the cyclic dimers

According to current thinking regarding the negative values of H_b as a covalency descriptor of interatomic interactions, the H-bonds of $(FA\text{-}X)_2$ complexes should be classified as a partially covalent interactions (since $\nabla^2\rho_b>0$ but $H_b<0$) [2, 10–13, 14, 16]. However, it has been argued recently that a negative value of H_b (or a trend towards negative values) is not necessarily associated with covalency or electrostatics but could be considered an indicator of strengthening or stabilization of the interaction, in the same way as a decrease in total interaction energy is an indicator of complex stabilization [7].

To get a clearer understanding about what the variations in H_b and other topological parameters mean during H-bond formation, we evaluated these parameters on the intermediate electron densities of $(FA\text{-}X)_2$ complexes derived from Morokuma analysis as implemented in the GAMESS electronic structure program (http://www.msg.ameslab.gov/gamess/). As indicated in Scheme 1, the total MP2 electron density of the complexes can be constructed as:

$$\{\rho(m_1)+\rho(m_2)\}+\Delta\rho_{ncov}+\Delta\rho_{cov}+\Delta\rho_{disp}=\rho^{MP2}(m_1,m_2) \quad (4)$$

The reader can find the values of the local topological parameters calculated on the $\{\rho(m_1)+\rho(m_2)\}$ density in the supporting information (Table S1). The $\{\rho(m_1)+\rho(m_2)\}$ density describes the monomer characteristics in its isolated state rather than in the H-bonded state. Hence, it is convenient to get rid of $\{\rho(m_1)+\rho(m_2)\}$ by subtracting it from the total MP2 electron density.

$$\Delta\rho_{ncov}+\Delta\rho_{cov}+\Delta\rho_{disp}=\rho^{MP2}(m_1,m_2)-\{\rho(m_1)+\rho(m_2)\} \quad (5)$$

In this way, the variation in the electron density of the monomers due to H-bond formation may be described in terms of the difference densities $\Delta\rho_{ncov}$, $\Delta\rho_{cov}$ and $\Delta\rho_{disp}$. In the following sections, discussion is focused on the study of the variation in topological parameters calculated from the $\Delta\rho_{ncov}$ and $\Delta\rho_{cov}$ difference densities. The topological parameters for the $\Delta\rho_{disp}$ difference density is not discussed further as the contribution from dispersion to total interaction energy is almost negligible for the systems studied here when compared with the other components (see Fig. 1).

Variations in charge density topological parameters from the $\Delta\rho_{ncov}$ difference density

Figure 2 shows the contour map of the $\Delta\rho_{ncov}$ difference density that accounts for the polarization or internal redistribution of the electronic charge within each monomer,

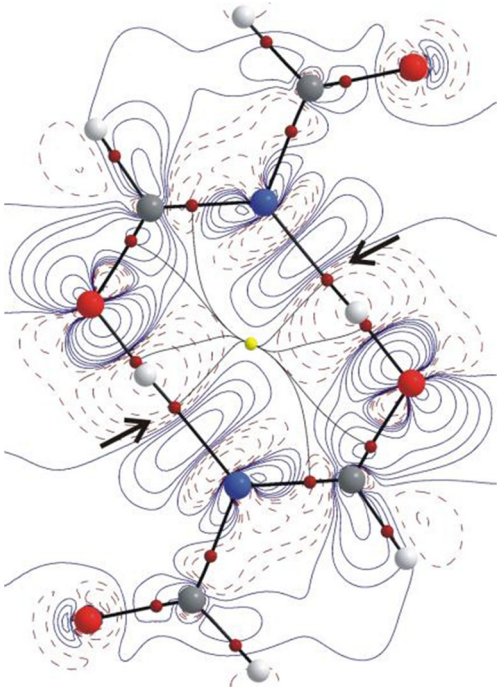

Fig. 2 Contour map of the $\Delta\rho_{ncov}$ difference density superimposed on the molecular graph of the $(AF\text{-}X)_2$ dimer; X = CHO. *Red dashed contour lines* Electron density decrease; *blue solid contour lines* electron density increase; *big circles* attractors or nuclear critical points (3, −3), attributed to nuclei; *lines connecting nuclei* bond paths,; *small red circles* bond critical points or (3, −1) critical points; *yellow circle* ring critical point; *arrows* H-bond critical points

superimposed on the molecular graph of the $(AF\text{-}X)_2$ dimer with X = CHO.

Two equivalent BCPs and the corresponding bond paths that connect both AF-CHO monomers can be observed in the graphs. It is a common feature of H-bonds that the H atom decreases its atomic population due to polarization of the H-donor bond X–H towards the donor X. In accordance with this statement, the $\Delta\rho_{ncov}$ contour map shows that the entire H basin decreases its charge density as a consequence of monomer polarization and, correspondingly, the H-donor oxygen atom increases its charge density. This polarization of the H-donor bond is complemented by a charge density shift of the H-acceptor basin toward the H atom. However, the H-donor polarization is more pronounced than that of the H-acceptor since the H-bond critical point becomes decreased in charge density after the monomers are allowed to polarize.

The overall result of the charge density redistribution on the H-donor bond and H-acceptor atom due to monomer polarization is that the electrostatic attraction between them is increased, as manifested by a decrease in the potential energy density at the H-bond critical point, as is shown below.

Table 2 reports the variations in the local topological parameters calculated from the $\Delta\rho_{ncov}$ difference density, for all $(FA\text{-}X)_2$ complexes, and Figs. 2 and 3 displays the

Table 2 Variations in the topological parameters[a] (in a.u.) from the $\Delta\rho_{ncov}$ difference density, in $(FA\text{-}X)_2$ complexes

X	$(\Delta\rho_b)_{ncov}$	$(\Delta¼\nabla^2\rho_b)_{ncov}$	$(\Delta G_b)_{ncov}$	$(\Delta H_b)_{ncov}$	$(\Delta V_b)_{ncov}$
F	−0.0035	0.0045	0.0059	−0.0015	−0.0074
NH_2	−0.0040	0.0049	0.0062	−0.0014	−0.0076
OH	−0.0042	0.0051	0.0064	−0.0013	−0.0077
CN	−0.0035	0.0057	0.0075	−0.0018	−0.0093
Cl	−0.0049	0.0066	0.0080	−0.0014	−0.0094
H	−0.0063	0.0081	0.0093	−0.0011	−0.0104
NO	−0.0053	0.0077	0.0094	−0.0017	−0.0110
CH_3	−0.0066	0.0087	0.0099	−0.0012	−0.0111
CHO	−0.0057	0.0087	0.0107	−0.0020	−0.0126

[a] The absolute values of the topological parameters are given in Table S1

corresponding difference contour maps for the $(AF\text{-}CHO)_2$ dimer, superimposed on the molecular graphs.

As with the AF-CHO dimmer, in the remaining complexes the electron density decreases in value at the H-bond critical point when each monomer is allowed to redistribute its charge density internally under the electric field of the other monomer, as indicated by the negative values of $(\Delta\rho_b)_{ncov}$ in Table 2. Furthermore, the $(\Delta\rho_b)_{ncov}$ value becomes in general more negative as the H-bond shortens, on going from X = F to X = CHO (see Table 1 for H-bond distances).

With regard to the local energy densities, the data in Table 2 as well as the difference contour maps in Fig. 3 show that the local potential energy density increases its negative value at the H-bond critical point $[(\Delta V_b)_{ncov}<0]$ and the local kinetic energy density becomes more positive at that point $[(\Delta G_b)_{ncov}>0]$ as a consequence of the monomers charge density polarization. The different behavior of the local potential and kinetic energy densities per electron charge might be seen as a consequence of the requirement for Heisenberg's uncertainty principle. The uncertainty principle seeks a balance between electrons having a low potential energy and not becoming confined in too small a space, which will lead to high kinetic energy (because of the uncertainly relation $\Delta p\ \Delta x \approx \hbar$) [21].

Since $|(\Delta V_b)_{ncov}| > (\Delta G_b)_{ncov}$, the total electronic energy density decreases in value $[(\Delta H_b)_{ncov}<0]$, namely, the decrease in local potential energy density drives the decrease in H_b (see Eq. 3). According to the usual meaning of the negativity of H_b as a covalency descriptor of H-bonds [2, 10–13, 14, 16], the observed decrease in H_b [or the $(\Delta H_b)_{ncov}$ negativity] might be interpreted as indicative of the increase in the covalence degree of the H-bond due to monomer polarization. However, this polarization, as computed in the Morokuma decomposition scheme, involves only an internal redistribution of charge density within each monomer. Therefore, the $(\Delta H_b)_{ncov}$ negativity could not be indicative of the increase in the covalence degree of the H-bond since the sharing of electrons between monomers is not allowed in the polarization

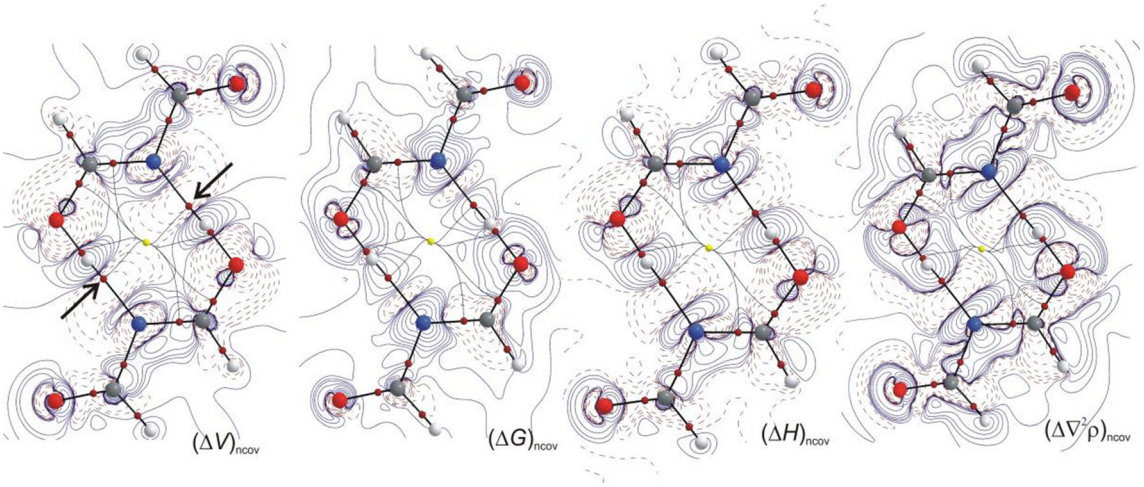

Fig. 3 Difference contour maps of the topological parameters superimposed on molecular graphs of the $(AF\text{-}CHO)_2$ dimer. $(\Delta V)_{ncov}$, $(\Delta G)_{ncov}$, $(\Delta H)_{ncov}$ and $(\Delta\nabla^2\rho)_{ncov}$ represent the changes in the potential, kinetic, and total electron energy densities and the Laplacian of electron density, respectively, as a consequence of monomer polarization. *Red dashed contour lines* Electron density decrease, *blue solid contour lines* electron density increase, *arrows* H-bond critical points

calculation. It has been argued recently that a negative value of H_b (or its trend towards negative values) is not necessarily associated with covalency or electrostatics but could be considered an indicator of the strengthening or stabilization of the interaction in the same way as the decrease in total interaction energy is an indicator of complex stabilization [7]. In accordance with this statement, the decrease in H_b [or $(\Delta H_b)_{ncov}$ negativity] in the $(FA\text{-}X)_2$ dimers describes properly H-bond strengthening due to monomer charge density internal redistribution or polarization.

In contrast to the H_b behavior, the Laplacian of charge density increases its value at the H-bond critical point $[(\Delta¼\nabla^2\rho_b)_{ncov}>0)]$, i.e., the H-bond critical point is depleted of charge density, evidencing the non-covalent character of the polarization component of the interaction energy (see Table 2 and Fig. 3).

Variations in the charge density topological parameters from the $\Delta\rho_{cov}$ difference density

Next, we analyzed the variations in topological parameters after sharing of electrons between monomers is "switched on". When the sharing of electrons between monomers is allowed, i.e., on going from the polarized to the total Hartree-Fock intermediate electron density (see Scheme 1), two components of the interaction energy come into play simultaneously: charge transfer (E_{CT}) and interelectronic repulsion (E_{EX}) between the monomers. Therefore, the density difference between these two intermediate electron densities, named as $\Delta\rho_{cov}$, accounts for the effect of the E_{CT} and E_{EX} components on the electron density of the monomers.

Figure 4 shows the contour map of the $\Delta\rho_{cov}$ difference density superimposed on the molecular graph of the $(AF\text{-}X)_2$ dimer with X = CHO.

Table 3 reports the changes in local topological parameters calculated from the $\Delta\rho_{cov}$ difference density for all the $(FA\text{-}X)_2$ complexes, and Figs. 4 and 5 displays the corresponding difference contour maps for the $(AF\text{-}CHO)_2$ dimer, superimposed on the molecular graph.

As can be seen in Table 3 and Fig. 4, the charge density at one of the equivalent H-bond critical points increases its value after the sharing of electrons between the monomers is

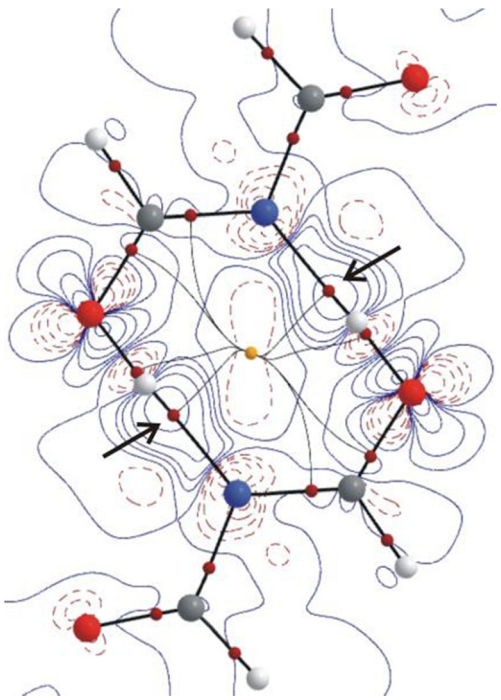

Fig. 4 Contour map of the $\Delta\rho_{cov}$ difference density superimposed on the molecular graph of the $(AF\text{-}X)_2$ dimer with X = CHO. *Red dashed contour lines* electron density decrease, *blue solid contour lines* electron density increase, *arrows* H-bond critical points

Table 3 Variations in the local topological parameters[a] (in a.u.) from the $\Delta\rho_{cov}$ difference density, in the $(FA\text{-}X)_2$ complexes

X	$(\Delta\rho_b)_{cov}$	$(\Delta¼\nabla^2\rho_b)_{cov}$	$(\Delta G_b)_{cov}$	$(\Delta H_b)_{cov}$	$(\Delta V_b)_{cov}$
F	0.0056	−0.0119	−0.0068	−0.0050	0.0018
NH_2	0.0053	−0.0118	−0.0071	−0.0047	0.0024
OH	0.0060	−0.0127	−0.0073	−0.0054	0.0019
CN	0.0070	−0.0150	−0.0084	−0.0066	0.0018
Cl	0.0075	−0.0164	−0.0091	−0.0073	0.0018
H	0.0092	−0.0202	−0.0111	−0.0092	0.0019
NO	0.0095	−0.0208	−0.0112	−0.0095	0.0017
CH_3	0.0099	−0.0217	−0.0118	−0.0099	0.0019
CHO	0.0109	−0.0241	−0.0129	−0.0112	0.0017

[a] The absolute values of the topological parameters are shown in Table S1

allowed [$(\Delta\rho_b)_{cov}>0$]. Furthermore, the $(\Delta\rho_b)_{cov}$ increment becomes more pronounced as the H-bond shortens, on going from X = F to X = CHO (see Table 1 for H-bond distances). The increase in the charge density at the H-bond critical point is accompanied by a decrease in the Laplacian of the electron density [$(\Delta¼\nabla^2\rho_b)_{cov}<0$] at that point (see Fig. 5). Since the $\Delta\rho_{cov}$ difference density accounts for the effect of the E_{CT} and E_{EX} components on the electron density of the monomers, the variation in topological parameters reflects the balance between these two opposing components (the charge transfer from the H-bond acceptor to the H-bond donor promotes electron density accumulation in the H-bonding region whereas the inter-electronic repulsion promotes the removal of charge density from that region). The observed decrease in $¼\nabla^2\rho_b$ together with the increase in ρ_b clearly indicates that the effect of E_{CT} on the electron density at the H-bond critical point prevails over the effect of E_{EX}, even when the value of the last energy component is generally greater in magnitude than the first (see Fig. 1). By inspecting the variations in the kinetic and potential energy densities (Table 3, Fig. 5) and taking into account the local virial theorem (Eq. 2), one can see that the negativity of $(\Delta¼\nabla^2\rho_b)_{cov}$ is driven by a decrease in the kinetic energy density [$(\Delta G_b)_{cov}<0$] since the potential energy density becomes less negative [i.e., $(\Delta V_b)_{cov}>0$] after the sharing of electrons between the monomers is "switched on". This decrease in G_b might be associated with the electron delocalization or charge transfer between the monomers through the uncertainly principle, which states that a decrease in the momentum leads to a more delocalized wavefunction, because of the uncertainly relation ($\Delta p\ \Delta x \approx \hbar$) [21]. Therefore, the decrease in G_b might be considered as the local manifestation (at the H-bond critical point) of the charge transfer between the monomers that promotes the charge density increase and the Laplacian decrease in the H-bonding region. On the other hand, the positive value of $(\Delta V_b)_{cov}$ is the local manifestation of the inter-electronic repulsion, which is secondary to the increase of electronic charge in the H-bonding region as a consequence of the charge transfer between the monomers.

Finally, $(\Delta H_b)_{cov}$ takes a negative value same as $(\Delta H_b)_{ncov}$, with the difference that the negativity of $(\Delta H_b)_{cov}$ is promoted by the decrease in G_b whereas the $(\Delta H_b)_{ncov}$ negativity is driven by the decrease in V_b.

Comparative analysis of the variations in the topological parameters from $\Delta\rho_{ncov}$ and $\Delta\rho_{cov}$ difference densities

Figure 6 shows stacked bars representing the topological parameters calculated on the $\{\rho(m_1) + \rho(m_2)\}$ density as well as the variations of these parameters from the $\Delta\rho_{ncov}$ and $\Delta\rho_{cov}$ difference densities, for the $(FA\text{-}X)_2$ complex with X = CHO. Similar variations were observed in complexes with different X substitution (see Tables 2, 3 and S1).

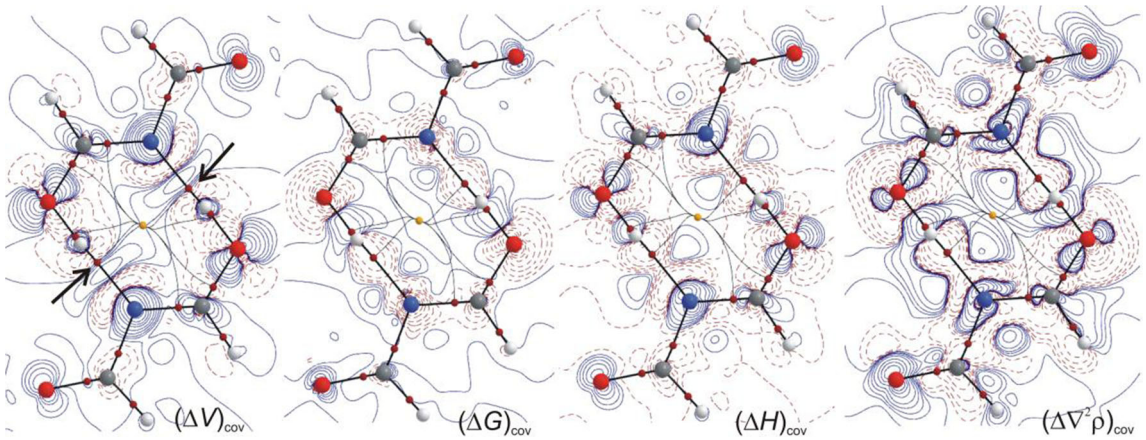

Fig. 5 Difference contour maps of topological parameters superimposed on the molecular graph of the $(AF\text{-}CHO)_2$ dimer. $(\Delta V)_{cov}$, $(\Delta G)_{cov}$, $(\Delta H)_{cov}$ and $(\Delta\nabla^2\rho)_{cov}$ are the changes in the potential, kinetic, and total electron energy densities and the Laplacian of electron density, respectively, after the differential overlap among monomers is allowed. *Red dashed contour lines* electron density decrease, *blue solid contour lines* electron density increase, *arrows* H-bond critical points

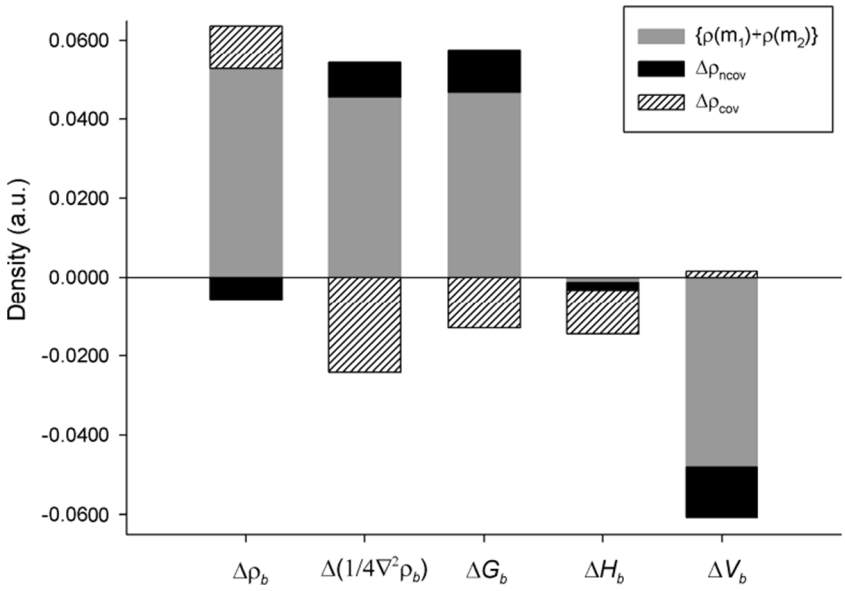

Fig. 6 Topological parameters on the $\{\rho(m_1) + \rho(m_2)\}$ density, and variations in these parameters from the $\Delta\rho_{ncov}$ and $\Delta\rho_{cov}$ difference densities, for the $(FA\text{-}X)_2$ complex with X = CHO

As was explained in a previous section, the $\{\rho(m_1) + \rho(m_2)\}$ density describes the monomer characteristics in its isolated state rather than in the H-bonded one, since it is computed as the sum of monomer densities in the complex geometry. It can be seen in Fig. 6 (and Tables 2, 3 and S1) that the values of the topological parameters on this density are in most cases bigger in magnitude than the variations of these parameters due to H-bond formation, namely the $\Delta\rho_{cov}$ and $\Delta\rho_{ncov}$ difference densities. This feature indicates that the engaged monomers preserve, to a large extent, the characteristics that they had in their isolated state, which is an expected result considering that H-bonds are closed shell interactions.

By analyzing the relative magnitude and sign of the variations of the topological parameters in Fig. 6, one can see how these parameters are modified with respect to the $\{\rho(m_1) + \rho(m_2)\}$ density after H-bond formation. Thus, for example, the potential energy density increases its negative value after H-bond formation (i.e., with respect to the $\{\rho(m_1) + \rho(m_2)\}$ density) since the negative variation $[(\Delta V_b)_{ncov}]$ due to polarization effects is greater in magnitude by far than the positive variation $[(\Delta V_b)_{cov}]$ due to interelectronic repulsion. This net increase in V_b negativity locally describes the electrostatic stabilization of the system after H-bond formation.

With regard to $¼\nabla^2\rho_b$ and G_b, the positive values of these terms decreases after H-bond formation due to the negative contributions of $(\Delta¼\nabla^2\rho_b)_{cov}$ and $(\Delta G_b)_{cov}$, which are greater in magnitude than the positive contributions $(\Delta¼\nabla^2\rho_b)_{ncov}$ and $(\Delta G_b)_{ncov}$, respectively. The net decrease in G_b and $¼\nabla^2\rho_b$ locally describes the increase in system electron delocalization after H-bond formation.

There is also a net electronic charge increase (with respect to the $\{\rho(m_1) + \rho(m_2)\}$ density) in the H-bonding region due to the positive value of $(\Delta\rho_b)_{cov}$, that outweighs the negative value of $(\Delta\rho_b)_{ncov}$. Because of the isomorphism that exists between the charge density and virial topologies [22], it is commonly said that the charge density is accumulated in the H-bonding region because it lowers the potential energy in that region, i.e., that it is mostly an electrostatic effect [23, 24]. However, we have shown that the driving force for the net increase in ρ_b after H-bond formation is not the lowering of V_b but the net decrease of G_b. In other words, the charge density increases in the H-bonding region not because it lowers the potential energy in that region but as a consequence of the electron delocalization or charge transfer between the monomers.

With regard to the total electronic energy density, H_b, it becomes more negative with respect to the monomers densities sum $\{\rho(m_1) + \rho(m_2)\}$. It can be seen in Fig. 4 that both $\Delta\rho_{ncov}$ and $\Delta\rho_{cov}$ difference densities contribute to this net decrease in H_b. Since these difference densities are very dissimilar in nature, the negative variations of H_b in both could not be considered as indicative of the increase in the covalence degree of the H-bond, as would be the case according to the current meaning of H_b negativity.

Conclusions

In this work, we have performed a charge density topological analysis on not only the total electron density of the complex but also on intermediate electron densities differences derived from the Morokuma energy decomposition scheme in order to gain insight into the meaning of the variation of the local topological parameters in the context of H-bond formation.

It was shown in a plausible way that the variations in the potential energy density at the H-bond critical point properly describe the electrostatics of H-bonding. Thus, the increase in

the negative value of V_b associated to the $\Delta\rho_{ncov}$ difference density locally describes the electrostatic attraction due to polarization effects, whereas the decrease in the negative value of V_b associated to the $\Delta\rho_{cov}$ difference density locally describes inter-electronic repulsion in the H-bonding region as a consequence of the sharing of electrons between monomers.

On the other hand, variations in the kinetic energy density at the H-bond critical point account for the localization/delocalization degree of the electrons. The observed increase in G_b after polarization is "switched on" is a consequence of the increased localization of the electrons due to a more negative V_b value. Conversely, the observed decrease in G_b associated with the $\Delta\rho_{cov}$ difference density locally describes the electron delocalization or charge transfer between the monomers.

It also has been shown that the net increase in the local charge density during H-bond formation is not related with the lowering of potential energy density in the H-bonding region but it is associated with electron delocalization after the sharing of electrons between monomers is allowed.

Finally, it was found that both $\Delta\rho_{ncov}$ and $\Delta\rho_{cov}$ difference densities contribute to the H_b decrease. We believe that, since these difference densities are very dissimilar in nature, the negative variations in H_b in both cases cannot be considered as indicative of an increase in the covalence degree of the H-bond, as would be the case according to the current meaning of H_b negativity. Instead, the negative values of $(\Delta H_b)_{ncov}$ and $(\Delta H_b)_{cov}$ properly describe the stabilization that the complexes experience due to polarization and delocalization effects, respectively.

Nevertheless, it must be noted that most of this decrease in H_b is related to electron delocalization in the H-bonding region, namely $(\Delta H_b)_{cov}$ is much larger than $(\Delta H_b)_{ncov}$, which might explain why this topological parameter is commonly considered as a covalence descriptor of these interactions. However, one cannot be sure that $(\Delta H_b)_{cov}$ will be much larger than $(\Delta H_b)_{ncov}$ in all cases without performing a density decomposition analysis such as that performed in this work.

Acknowledgment We acknowledge the Secretaría de Ciencia y Tecnología de la Universidad Nacional del Nordeste (SECYT UNNE) and Consejo Nacional de InvestigacionesCientíficas y Técnicas (CONICET) for financial support. The authors also acknowledge the use of CPUs from the High Performance Computing Center of the Northeastern of Argentina (CECONEA). This work was supported by the Grants PIP 095 CONICET and 2010F023 SECYT-UNNE.

References

1. Pauling L (1960) The nature of the chemical bond. Cornell University Press, Ithaca
2. Grabowski SJ (2011) What is the covalency of hydrogen bonding? Chem Rev 111(4):2597–2625. doi:10.1021/cr800346f
3. Morokuma K (1977) Why do molecules interact? The origin of electron donor-acceptor complexes, hydrogen bonding and proton affinity. Acc Chem Res 10(8):294–300. doi:10.1021/ar50116a004
4. Morokuma K, Kitaura K (1981) Energy decomposition analysis of molecular interactions. In: Politzer P, Truhlar DG (eds) Chemical applications of atomic and molecular electronic potentials. Plenum, New York, pp 215–242
5. Clark T (2013) σ-holes. WIRES Comput Mol Sci 3(1):13–20. doi:10.1002/wcms.1113
6. Politzer P, Riley KE, Bulat FA, Murray JS (2012) Perspectives on halogen bonding and other σ-hole interactions: Lex parsimoniae (Occam's Razor). Comput Theor Chem 998:2–8. doi:10.1016/j.comptc.2012.06.007
7. Angelina EL, Duarte DJR, Peruchena NM (2013) Is the decrease of the total electron energy density a covalence indicator in hydrogen and halogen bonds? J Mol Model 19(5):2097–2106. doi:10.1007/s00894-012-1674-y
8. Bader RWF (1990) Atoms in molecules: a quantum theory. Oxford University Press, New York
9. Angelina EL, Peruchena NM (2011) Strength and nature of hydrogen bonding interactions in mono- and di-hydrated formamide complexes. J Phys Chem A 115(18):4701–4710. doi:10.1021/jp1105168
10. Jenkins S, Morrison I (2000) The chemical character of the intermolecular bonds of seven phases of ice as revealed by ab initio calculation of electron densities. Chem Phys Lett 317(1–2):97–102. doi:10.1016/S0009-2614(99)01306-8
11. Arnold WD, Oldfield E (2000) The chemical nature of hydrogen bonding in proteins via NMR: J-couplings, chemical shifts, and AIM theory. J Am Chem Soc 122(51):12835–12841. doi:10.1021/ja0025705
12. Espinosa E, Alkorta I, Elguero J, Molins E (2002) From weak to strong interactions: a comprehensive analysis of the topological and energetic properties of the electron density distribution involving X–H···F–Y systems. J Chem Phys 117(12):5529–5542. doi:10.1063/1.1501133
13. Pakiari AH, Eskandari K (2006) The chemical nature of very strong hydrogen bonds in some categories of compounds. J Mol Struct THEOCHEM 759(1–3):51–60. doi:10.1016/j.theochem.2005.10.040
14. Grabowski SJ, Sokalski WA, Dyguda E, Leszczyński J (2006) Quantitative classification of covalent and noncovalent H-bonds. J Phys Chem B 110(13):6444–6446. doi:10.1021/jp0600817
15. Esrafili M (2012) Characteristics and nature of the intermolecular interactions in boron-bonded complexes with carbene as electron donor: an ab initio, SAPT and QTAIM study. J Mol Model 18(5):2003–2011. doi:10.1007/s00894-011-1221-2
16. Grabowski SJ, Sokalski WA, Leszczynski J (2006) The possible covalent nature of N-H···O hydrogen bonds in formamide dimer and related systems: an ab initio study. J Phys Chem A 110(14):4772–4779. doi:10.1021/jp055613i
17. Grabowski S (2009) Covalent character of hydrogen bonds enhanced by π-electron delocalization. Croat Chem Acta 82(1):185–192
18. Frisch MJ, Trucks GW, Schlegel HB, Scuseria GE, Robb MA, Cheeseman JR, Montgomery JA Jr., Vreven T, Kudin KN, Burant JC, Millam JM, Iyengar SS, Tomasi J, Barone V, Mennucci B, Cossi M, Scalmani G, Rega N, Petersson GA, Nakatsuji H, Hada M, Ehara M, Toyota K, Fukuda R, Hasegawa J, Ishida M, Nakajima T, Honda Y, Kitao O, Nakai H, Klene M, Li X, Knox JE, Hratchian HP, Cross JB, Adamo C, Jaramillo J, Gomperts R, Stratmann RE, Yazyev O, Austin AJ, Cammi R, Pomelli C, Ochterski JW, Ayala PY, Morokuma K, Voth GA, Salvador P, Dannenberg JJ, Zakrzewski G, Dapprich S, Daniels AD, Strain MC, Farkas O, Malick DK, Rabuck AD, Raghavachari K, Foresman JB, Ortiz JV, Cui Q, Baboul AG, Clifford S, Cioslowski J, Stefanov BB, Liu G, Liashenko GA,

Piskorz P, Komaromi I, Martin RL, Fox DJ, Keith T, Al-Laham MA, Peng CY, Nanayakkara A, Challacombe M, Gill PMW, Johnson B, Chen W, Wong MW, Gonzalez C, Pople JA (2004) Gaussian 03, revision D01; Gaussian, Inc, Wallingford

19. Schmidt MW, Baldridge KK, Boatz JA, Elbert ST, Gordon MS, Jensen JH, Koseki S, Matsunaga N, Nguyen KA, Su S, Windus TL, Dupuis M, Montgomery JA (1993) General atomic and molecular electronic structure system. J Comput Chem 14(11):1347–1363. doi:10.1002/jcc.540141112
20. Keith TA (2012) AIMAll (Version 12.11.09). TK Gristmill Software, Overland Park, KS (http://aim.tkgristmill.com/)
21. Feynman RP, Leighton RB, Sands M (1964) The Feynman lectures on physics. Addison-Wesley, Reading
22. Bader RFW (1998) A bond path: a universal indicator of bonded interactions. J Phys Chem A 102(37):7314–7323. doi:10.1021/jp981794v
23. Bader RFW, Henneker WH, Cade PE (1967) Molecular charge distributions and chemical binding. J Chem Phys 46(9):3341–3363
24. Bader RFW, Preston HJT (1969) The kinetic energy of molecular charge distributions and molecular stability. Int J Quantum Chem 3(3):327–347. doi:10.1002/qua.560030308